Ion Thruster Thrust Vectoring Requirements and Techniques

David G Fearn
Space Department,
QinetiQ,
Farnborough,
Hants, GU14 0LX, UK
(44)-1252-392963
dgfearn@scs.dera.gov.uk

IEPC-01-115

In any spacecraft installation of an ion propulsion system it is likely that there will be a need to alter the position of the thrust vector with respect to the centre of mass, in order to minimise attitude and orbital perturbations during operation. In addition, this offers a possible means of direct attitude control, or of unloading momentum wheels and similar devices. This control of the thrust vector is normally accomplished using a mechanically actuated gimbal platform. As such devices are heavy and expensive, and may suffer from reliability problems, alternatives are worthy of consideration. This paper reports a study of these alternatives, which include mechanical, plasma, electrostatic and electromagnetic options. Although the plasma principle, in which the plasma density distribution in the discharge chamber is changed to provide an offset thrust vector, shows promise, it must be regarded as a long-term. Of the relatively short-term concepts available, the electrostatic vectoring of the emerging ion beam, by moving one of the extraction grids laterally, is inherently the most effective.

Introduction

Many different electric propulsion (EP) systems are under development, employing a wide variety of electrostatic, electromagnetic and electrothermal acceleration mechanisms [1]. In each case, an energetic beam of ionised propellant is ejected from the engine, providing the required momentum transfer and thrust. The properties of this beam include the position and stability of the thrust vector, which are very important to the design and operation of the attitude and orbit control system (AOCS) of the spacecraft. At any particular time, this vector is determined by the spatial and angular distributions of the particles constituting the beam and by their individual energies, which are not easily measured as independent parameters.

Ideally, the position of the thrust vector relative to the centre-of-mass (CoM) of the spacecraft should be known precisely at all times to allow the design and operation of the AOCS to be optimised to minimise the consumption of propellant by the chemical thrusters employed to correct the orbit and attitude of the spacecraft, or to unload any momentum wheels carried for attitude control. However, even if this was achieved, propellant consumption would substantial, owing to inevitable uncertainties in the position of the CoM. These are due to the reducing amount of propellant in the tanks and to the movements of solar arrays and other appendages, as well as to original design and manufacturing tolerances.

To compensate for this uncertain geometrical relationship between thrust vectors and the CoM of the spacecraft, a gimbal system must be provided to permit the exhausts of the thrusters to be directed so as to minimise disturbance forces and torques. As an example, this technique is used on ESA's Artemis communications spacecraft [2]. An alternative in certain applications might be to throttle thrusters selectively to attain the same objective, although this concept has not so far been applied in practice.

It should be noted that a thrust vectoring system can also be used directly for attitude control of the

Presented as Paper IEPC-01-115 at the 27th International Electric Propulsion Conference, Pasadena, CA, 15-19 October, 2001.

spacecraft. However, although a valuable means by which propellant consumption can be reduced further, this cannot replace the AOCS thrusters, since the EP system will not, in general, be operating continuously. It is probably more useful to employ the thrusters to offload any momentum wheels employed for attitude control; this option has been adopted for the Boeing/Hughes HS-702 platform [3].

There are several disadvantages associated with the use of gimbals. The most important concern mass and cost, since they tend to be expensive and relatively large and heavy. In addition, being mechanical systems with moving parts, there is concern regarding their reliability over long duration missions. There is, as a consequence, considerable interest in replacing them by alternative methods of thrust vectoring.

In the context of gridded ion thrusters, the need for non-mechanical vectoring techniques has been recognised for many years [4-6], especially for the north-south station-keeping (NSSK) application in geostationary Earth orbit (GEO). Many possible concepts has been suggested and, in some cases, explored experimentally. Examples include the use of high electric [5, 7] or magnetic fields [7] to deflect the beam from a thruster through an appropriate angle, and the electrostatic deflection of the beam by relative translational movements between the extraction grids [4, 6]. Unfortunately, none of these ideas have so far proved to be operationally viable.

These methods are reviewed in this paper, following a more detailed discussion of requirements, and it is again concluded that most of them are not likely to be successful, particularly for very long duration missions. However, recent advances in a number of areas of technology suggest that there is merit in a careful re-examination of the grid translation concept. In addition, a new approach to this requirement has been suggested which involves the deliberate distortion of the density distribution of the energetic particle flux in the beam emitted by a gridded ion thruster, thereby offsetting the thrust vector from the centreline. This requires only electrical actuation, but must be regarded as a long-term possibility.

NSSK Thrust Vectoring Requirements

Spacecraft Design and Configuration

In order to evaluate thrust vectoring requirements, certain assumptions must be made about the spacecraft configurations and thruster mounting arrangements likely to be used. Although various studies [8-10] have examined the possibility of adding an ion propulsion system (IPS) to an existing platform, it is generally considered advantageous to design any spacecraft likely to use an IPS with this possibility in mind from the outset if the maximum benefits are to be obtained [10]. In this process, all tasks for which the thrusters might be used should be considered; these could include east-west station-keeping (EWSK) and de-orbit at the end of the mission [11].

In the same way, all appropriate thruster-spacecraft interactions [12] should be taken into account. As already described, the thrust vector stability is important to the design of the AOCS and to the amount of chemical propellant that might need to be carried for attitude control. Of equal significance are the ion beam divergence and the way in which material sputtered from the thruster is likely to be deposited on sensitive surfaces, such as solar arrays and thermal control panels. These characteristics largely define the overall spacecraft configuration, since a highly diverging beam will interact with solar arrays aligned along the north-south (NS) axis.

Assuming the use of conventional gridded ion thrusters, with beam divergence half-angles in the range 10 to 20 deg [12], the spacecraft configurations shown in Fig 1 are usually advocated, although many others are also possible. They are appropriate to solar arrays designed to rotate around the NS axis of the spacecraft, with ϕ defined as the angle between the mean thrust vector and this axis. Clearly, the thrust vector stability to some extent determines the value of this parameter, which must be selected to avoid direct ion beam impingement on the solar arrays.

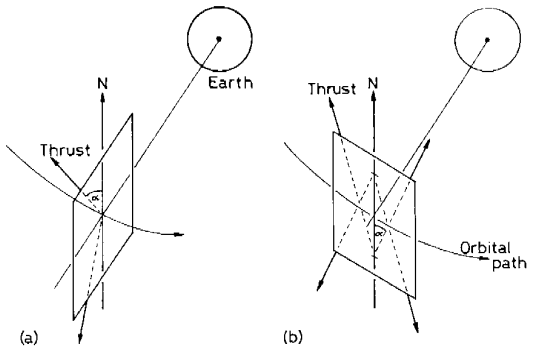

Figure 1 – Two possible thruster mounting configurations for NSSK: a. Radial b. Tangential.

In the layout illustrated in Fig 1b, two thrusters must operate simultaneously and their thrusts must balance,

if attitude perturbations are to be avoided. This necessitates the use of precise throttling over a limited range, which is possible with most gridded thrusters, such as the UK-10 system [13], the Melco thrusters [14] used on the ETS-VI spacecraft, and the RIT-10 device [15]. This can be readily implemented using an appropriate output from the AOCS computer as the IPS control parameter.

The radial mounting configuration adopted for Artemis [2] was unique at the time of its adoption, in that it permits one thruster at a time to be used, enhancing the redundancy of a 4-thruster installation, and halving the power required (although doubling the operating time to produce a given orbital effect). This scheme is that shown in Fig 1a. With single thrusters operating through the CoM in the radial direction, the unbalanced force is towards the Earth. It causes a slight change in the eccentricity of the orbit, which can be compensated for by an initial distortion of only about 400 m in altitude [16].

Although there are several viable options when considering spacecraft configuration and design, the greatest mass benefits from using an IPS for NSSK accrue when the minimum possible value of ϕ is adopted. This tends to disadvantage the unique Artemis layout and to favour those similar to that shown in Fig 1b. Conversely, the latter have the disadvantages of lower effective redundancy and the need to operate two thrusters simultaneously. As regards overall reliability, the Artemis concept is usually judged to be superior to the alternatives.

Orbital Perturbations

As pointed out above, in designing the installation and operational strategy for the IPS, consideration should be given to the orbital perturbations that might result from its use. Although such perturbations occur with any propulsion system, the characteristics of an IPS are very different from those of conventional chemical thrusters, necessitating a re-examination of this question. In particular, the thrust levels are usually much lower in the case of the IPS, leading to considerably smaller perturbing forces and torques. Conversely, these forces and torques are applied for hours, rather than minutes or seconds. As a consequence, the control philosophy employed will be different in the two cases. In this context, it is worth pointing out the intrinsic safety of using such low thrusts; if a problem occurs, the adverse results will develop only slowly and there will usually be adequate time in which to take remedial action. This is not the case with relatively high thrust chemical systems.

In examining orbital perturbations due to the IPS, the tangential and radial mounting strategies must be treated separately. With thrusting in the plane tangential to the velocity vector (Fig 1b), the main perturbation is any imbalance of the thrust component in the east-west (EW) direction; indeed, such an imbalance can be usefully employed for EWSK and spacecraft repositioning [17]. In the other configuration, with thrusting in the plane containing the spacecraft-Earth vector, any out-of-balance force influences only the eccentricity of the orbit [16].

In early studies of orbital perturbations caused by the use of an IPS [8, 18], two of the most important parameters, the thrust vector misalignment and thrust vector stability, were unknown for any of the candidate ion engines. Measurements had not been made in most cases and, even where some data were available, the precision was poor. As a result, it had to be assumed that both parameters were of the order of 3 deg. In addition, errors due to thrust imbalances had to be considered.

As an example of the repercussions of such misalignments and imbalances, the results of an analysis conducted at the time can be re-visited. In this worst-case analysis of a comsat of 750 kg mass [8], it is assumed that all thrusters used for NSSK have similar characteristics and that the misalignments reinforce each other. The thrust component perpendicular to the NS direction is then 6.4×10^{-4} N. This gives rise to an average velocity increment of 2.6×10^{-3} m/s per day, which is in the EW direction for the spacecraft in Fig 1b. If the disturbances due to the two pairs of thrusters facing in opposite directions are not correlated, the square root of the sum of the squares (SRSS) of the individual perturbations will give a measure of the overall effect. This gives an average velocity increment per day of 3.7×10^{-3} m/s.

As regards the provision of unequal thrusts by the two devices constituting a pair, the mismatch is assumed to be of the order of ± 3%. Taking the worst case of the two thrusters mounted on one face (north or south) of the spacecraft being 3% high and 3% low, the force perpendicular to the north-south axis is found to be 2.1×10^{-4} N. The equivalent average daily velocity increment is then 8.5×10^{-4} m/s. Using the SRSS process, the velocity increment per day due to both pairs of thrusters is 1.2×10^{-3} m/s.

Combining both of these sources of error, the SRSS velocity increment per orbit, ΔV_p, becomes 3.8×10^{-3} m/s. This is either along the spacecraft's velocity

vector or in the perpendicular direction, depending upon which of the configurations shown in Fig 1 is considered.

In the tangential case, if the semi-major axis is a, its perturbation is given by $\Delta a = 2\Delta V_p/\omega$, where ω is the angular velocity of the orbit. In the case analysed, Δa is 106 m. For an initially geosynchronous orbit, this leads to a longitudinal drift rate of 1.36×10^{-3} deg per day, with no change in eccentricity, assuming that the error is the same on both sides of the orbit. If the errors are in opposite senses around the two nodes, there will be no net change in a and thus zero drift. There will, however, be an eccentricity change $\Delta e_o = 2\Delta V_p/v_o$, where v_o is the orbital velocity, which amounts to 2.5×10^{-6}. This causes a daily libration about the mean satellite longitude of 3×10^{-4} deg, which can be ignored.

It is evident that the most important effect is upon the orbit semi-major axis, and thus on the satellite's longitudinal drift rate. If the EWSK cycle time is long, coupling from the daily NS manoeuvre can lead to a significant satellite drift. This results in a noticeable increase in the propellant budgets for the chemical thrusters usually employed for EWSK. The alternative is to provide a thrust vectoring system to counteract these and the associated attitude errors.

To give an example of the quantities of propellant involved, the above analysis has been repeated for a satellite in the Intelsat VII class [19, 20], which has a dry mass of close to 1500 kg. Assuming the use of bi-propellant thrusters with a specific impulse (SI) of 285 sec, the propellant consumptions are as follows, for a mission duration of 15 years:

Vector error only	10.9 kg
Thrust imbalance only	3.5 kg
SRSS combination of above	11.2 kg

It is clear that a mass penalty of this order will not be a major problem for a large communications satellite, so that thrust vector errors of up to 3 deg and thrust inequalities of 3% are acceptable. As gridded thrusters are now known to provide a thrust vector stability of better than 0.1 deg [21] and thrust control of much better than 1% is readily achievable [22], these mass values are unduly pessimistic, by nearly an order of magnitude, and suggest that active vectoring may not be necessary for this purpose alone.

If ΔV_p is purely radial (Fig 1a), and noting that e_o is very small, the maximum perturbation is

$$|\Delta a| \approx \left| \frac{2 e_o \Delta V_p}{\omega} \right|$$

Due to the fact that the eccentricity is very small for a nearly circular synchronous orbit, this can be ignored. The accompanying perturbation to e_o is $\Delta e_o = \Delta V_p/v_o = 1.3 \times 10^{-6}$, which is also negligible.

It can be concluded that orbital perturbations due to thrust vector errors and thrust imbalances may need correction only if the thrusters are mounted in the tangential plane, as in Fig 1b, but that changes in a and e_o are certainly negligible if radial mounting is employed (Fig 1a).

The case of the failure of one thruster of a pair is also relevant. In the tangential mounting scheme, the resulting thrust imbalance in the EW direction is 5×10^{-3} N, which will, if not corrected, produce an average daily EW velocity increment of 0.04 m/s. This gives rise to a change of 1 km in the semi-major axis per day and an associated longitudinal drift rate of 0.014 deg, which is certainly unacceptable. In the case of the other mounting configuration, the coupling effects are again much less severe and can be ignored.

These results suggest that radial mounting is to be preferred, despite the disadvantage of the large value of ϕ needed in most applications. It was as a result of an assessment of this kind that ESA decided to choose the radial configuration for Artemis [2], since they did not, at the time, have any firm information concerning thrust vector direction and stability, and thrust variations for the candidate thrusters. However, more recent analysis [16] has shown that the effects on the spacecraft orbit can be reduced further, by introducing a small departure of only about 400 m from true GEO.

Following such analyses, most concerns about the impact of an IPS on orbit control in the EW and radial directions have been dispelled. It can now be assumed that additional propellant for correcting these perturbations will be negligible for configurations involving the balance of the thrusts produced by two engines. This is, of course, only the case if the engines give nearly identical thrusts within a few percent, or if they have an active throttling capability. The radial configuration (Fig 1a) is much less sensitive to such imbalances, and far less precise control is needed.

Attitude Perturbations

During station-keeping, disturbance torques will be

generated by thrust vector misalignments and instabilities, by thrust imbalances, and by movements of the CoM of the spacecraft. The first three causes have been considered above in the context of orbital perturbations and have been shown to be far less serious than originally thought. Movements of the CoM are due to several sources, but principally to changes in the contents of the propellant tanks. Other causes include the rotation of the solar arrays and movements of other appendages, and thermal distortions of these components and of the structure.

Such disturbance torques must be counteracted by the attitude control system (ACS), ultimately using chemical propellant. Alternatively, active thrust vector control of the ion thrusters might be considered, although the use of gimbal mounts for this purpose, as employed on Artemis [2], is a relatively heavy and costly solution to this requirement.

The mass penalty due to a thrust vector misalignment γ can be assessed using the theoretical treatment presented originally by Pye [18]. Following this analysis for the case of the radial mounting configuration (Fig 1a), if the misalignment of a thruster of thrust F is orientated to give the maximum torque about the yaw axis, this torque is $Fl\sin\gamma$, where l is the distance between the planes containing the thruster and the CoM (Fig 2). Assuming that an SRSS calculation gives the net torque produced by a pair of thrusters, this becomes $T_y = \sqrt{2}Fl\sin\gamma$, and the total angular impulse over the mission is

$$I_y = \left(\sqrt{2}Fl\tau\sin\gamma\right)/2 \qquad (1)$$

where τ is the total thrusting time during the mission. In cases in which two thrusters operate simultaneously, each will require a lifetime of $\tau/2$. Since thrusting occurs around opposite nodes of each orbit, a further SRSS calculation gives the angular impulse applied throughout the mission, which is

$$I_{yT} = Fl\tau\sin\gamma \qquad (2)$$

As an example of the magnitude of this parameter, with F = 25 mN, l = 1 m, γ= 0.1 deg, and τ = 10,000 hr, I_{yT} = 1570 Nsm. If a value of γ of better than 1 deg could not be achieved, I_{yT} would increase by a factor of 10.

Although equ (1) also applies to misalignments about the roll axis, a similar analysis shows that the angular impulse developed about the pitch axis by a pair of thrusters over the mission is

$$I_p = \sqrt{2}Fl\tau\tan\phi\tan\gamma$$

Similar results to those of equ (1) apply in the case of the tangential mounting arrangement in Fig 1b, but with the thruster positions transposed. It is also possible to treat in this way the torques generated by any misalignment of the thrust vector, or movement of the CoM of the satellite, in the single thruster operating scheme adopted for Artemis [2].

To evaluate the mass penalty implied by the derived total angular impulse, the geometry of the spacecraft must be known, in particular the moment arms of any thrusters employed, also the method of implementing attitude control. If this is done in real-time, using, for example, hydrazine thrusters, the effective SI will be quite low and the resulting propellant consumption correspondingly large. For example, if the SI, denoted by I_{sp}, is 200 sec and the thruster moment arms are 1.5 m long, the propellant consumptions corresponding to the values of I_{yT} quoted above are between 0.5 kg and 5 kg. If I_{sp} is reduced to 100 sec, this is 1 to 10 kg.

While acceptable, these values refer to ion engines with thrust vectors that are not misaligned by more than 0.1 deg, implying characterisation to an accuracy of better than this figure. If the thrust vector misalignments are significantly worse than this, the propellant consumption will be much greater. For example, as the total angular impulse is proportional to γ for small angles (equ 2), the propellant mass required will rise to between 50 and 100 kg for γ= 1 deg. This is not acceptable, and illustrates the importance of this parameter in the context of attitude control.

If momentum wheels are used, the chemical thrusters will have to operate only infrequently and for longer periods of time in order to desaturate the wheels. They will therefore operate more efficiently, with a higher SI, and the propellant mass required will be reduced. However, this gain must be balanced against the mass and complexity of the momentum wheel system, and any resultant impact on reliability.

The contribution made to disturbance torques by thrust vector instabilities can be considered in the same way as above. However, since changes in the thrust vector during steady-state operation of the T5 thruster are usually less than ± 0.02 deg [23], this can be neglected, assuming that all gridded engines have similar characteristics. This is a considerable improvement over the situation which existed at the time the decision was made to fly an IPS on the

Artemis satellite [24], when it was thought that the thrust vector might vary by as much as 3 deg.

As regards possible thrust imbalances between pairs of thrusters operating simultaneously in the configuration of Fig 1b, they will produce an unwanted torque, which must be corrected by the ACS. The magnitude of this effect will depend on the accuracy with which the power conditioning and control equipment (PCCE) regulates the thrust if active throttling is not employed. With throttling, a real-time control loop receiving error signals from the ACS can eliminate this source of attitude disturbance. It can also be used, during NSSK operations, to correct for other unwanted torques.

If the thrusts produced by a pair of engines differ from nominal by ΔF, such that they become $(F + \Delta F)$ and $(F - \Delta F)$, the effective torque due to this imbalance is

$$T_t = \sqrt{2}\Delta F L \sin\phi$$

where L is the distance between the CoM and the point of intersection of the thrust vectors. If both pairs of thrusters operate for the complete mission, with a misalignment γ also taken into account, the total angular impulse becomes

$$I_{tT} = \Delta F l \tau \tan\gamma \tan\phi$$

having substituted

$$L = l \tan\gamma / \cos\phi \qquad (3)$$

If ΔF = 0.03F, l = 1 m, τ = 10,000 hr, ϕ = 30 deg, and γ = 0.1 deg, I_{tT} becomes 40 Nsm and the propellant consumption is tiny, at only 15 g, assuming moment arms of 1.5 m and an SI of 200 sec. If a larger value of γ is more appropriate, say 1 deg, this consumption is increased to 140 g, which can also be ignored.

Movements of the CoM

As mentioned above, an offset in the CoM can be treated similarly to thrust vector misalignments, with γ being obtained from equ (3). Taking the parameters used previously, and assuming an offset of 1 cm, the resulting propellant consumption for the complete mission is 26 kg. This is of serious concern, since the CoM is likely to move through much larger distances, bearing in mind the size of modern communications satellites and the propellant loads carried by them[19]. It can therefore be concluded that thrust vectoring is required to compensate for movements in the CoM, no matter what form of EP system is used for station-keeping. Indeed, this effect dominates.

It is instructive to determine the angle through which the thrust vector would need to be changed to provide compensation for all movements of the CoM. This was assessed assuming the spacecraft configuration illustrated in Fig 2. In this, the nominal thrust vector passes through the centre of the body of the vehicle, where it is assumed that the CoM would normally be located. As a typical example, the thruster shown is mounted at one corner at an angle ϕ to the NS axis, with its grids protruding distance p from the corner. The thrust is taken to be generated at the centre of the grid system, which is a distance s from the right-hand face of the spacecraft and r from the north face.

For simplicity, only one axis is considered, with the CoM moving distance d in the NS direction only. This corresponds to a change in the angle with which a compensating thrust vector meets the horizontal axis from θ_1 to θ_2. Clearly, a similar treatment for the other two axes permits motion in any direction to be evaluated.

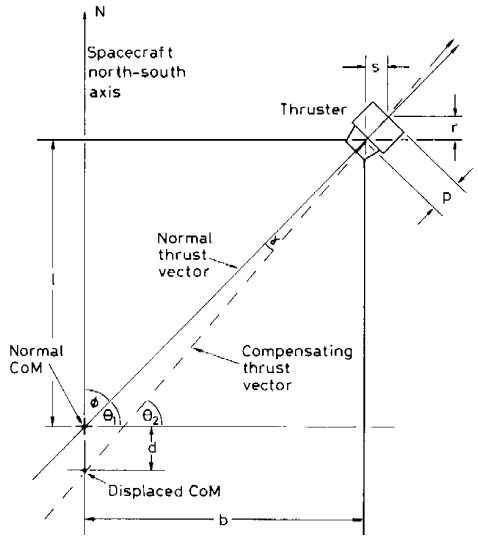

Figure 2 – Thruster mounting configuration, showing movement of the CoM.

If the change in thrust vector direction corresponding to the movement d in the CoM is α, and the half-width of the body of the spacecraft is b,

$$\tan\alpha = \frac{\tan\theta_2 - \tan\theta_1}{1 + \tan\theta_1 \tan\theta_2}$$

where $\tan\theta_1 = l/b$ and $\tan\theta_2 = \dfrac{l + d + p\cos\phi}{b + p\sin\phi}$.

As a realistic example, the case of the Intelsat VII

spacecraft, if fitted with an IPS, was considered[20]. Assuming that the Artemis thrusting strategy would be used, with 10 cm beam diameter thrusters mounted on the centres of the anti-Earth north and south corners of the body of the satellite, reasonable values of the geometrical parameters are p = 5 cm, l = 110 cm, and b = 130 cm. Thus ϕ = 50 deg, assuming that the CoM is in the geometrical centre of the spacecraft; although an undesirable angle from the point of view of thrusting efficiency, this is necessitated by the shape of the body of the spacecraft.

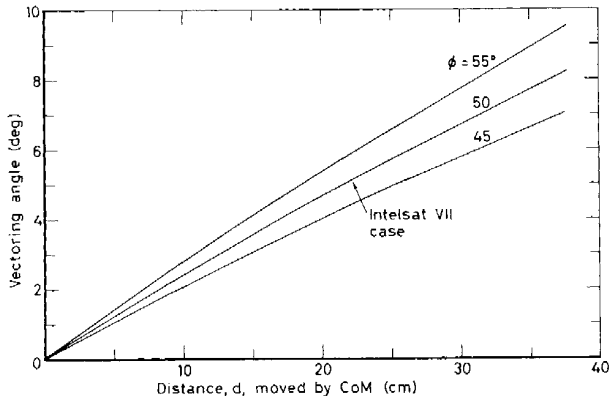

Figure 3 – Thrust vectoring angle as a function of the distance moved by the CoM of the satellite.

Using these dimensions and the above expressions, the values of α plotted against d in Fig 3 were obtained. It can be seen that there is an almost linear relationship between these parameters for the relatively small values of d considered. These angles cover the range 0 to 7 deg for CoM movements of up to 30 cm, indicating the degree of thrust vectoring required.

To assess the impact of the geometrical shape of the body of the spacecraft, two additional values of ϕ were examined, 45 and 55 deg. The results, shown in Fig 3, indicate that the overall effect is not large. To accommodate all geometries investigated, and values of d of up to 30 cm, a maximum vectoring angle of 8 deg is required. This value was assumed in the remainder of the study.

Practical Considerations

In the analysis presented above, it has been assumed in calculating propellant masses that exact attitude corrections are possible by using small chemical thrusters, probably using propellants also employed in the apogee boost motor. However, since these thrusters will have been designed for attitude control applications in which NSSK and EWSK are performed by other chemical thrusters, with thrusts of the order of 10 to 20 N, the minimum impulse bit available may be too large for the corrections now required. There may thus be an over-correction when one of these thrusters is fired, and the satellite will rotate to the other side of the allowable error band, necessitating a further firing in the opposite direction. This oscillatory rotation is likely to continue while the IPS is operating, causing propellant to be wasted.

A solution to this problem would be to fly thrusters with a much lower minimum impulse bit. Apart from smaller bi-propellant or hydrazine thrusters, other possibilities include cold gas thrusters, pulsed plasma thrusters, and field-emission thrusters. In addition, it should be noted that many spacecraft utilise momentum wheels for attitude control. Although these are not usually orientated to absorb the unwanted angular momentum introduced during NSSK operations, so cannot immediately solve the problem outlined above, the system could be re-designed for this purpose. This would, of course, add complexity and cost.

It can be concluded that the very small disturbing torques introduced by ion thrusters employed for NSSK are not as benign as indicated by simple calculations of the propellant masses required for their correction. When the minimum impulse bits of existing ACS thrusters are considered, these masses increase, reinforcing the need for thrust vectoring.

It is clear that any movement of the CoM, followed in importance by thrust vector misalignments, are potentially the most significant causes of AOCS propellant consumption due to the employment of an IPS on a comsat. However, in earlier work [8] it was assumed that $\gamma \approx 3$ deg, since no other information was available at the time. Precise values for this parameter are now available for gridded thrusters [21, 23], and a more appropriate angle is 0.1 deg, a factor of 30 improvement. As a consequence, the previous concern about the impact of an IPS on the AOCS has been somewhat alleviated, although movements of the CoM remain of considerable significance.

It can be concluded that thrust vectoring is not normally required to compensate for thrust vector misalignments and instabilities in typical gridded ion engines. The main reason for including a vectoring capability is to compensate movements of the CoM of the spacecraft. The vectoring angles involved depend on the detailed design of the spacecraft, but for a configuration of the type represented by Intelsat VII

and a displacement of the CoM by up to 30 cm along the NS axis, the maximum angle required is about 8 deg. Bearing in mind that this displacement can also occur along the axes perpendicular to the NS direction, vectoring in these directions is also required.

Vectoring Mechanisms

Principles

The relatively small vectoring angle identified above suggests that electromagnetic or electrostatic processes might be used. The simplest way of approaching this would be to apply magnetic or electric fields to the ion beam as it emerges from the grids of the thruster, to deflect it through the required angle. These possibilities are the first to be considered below.

As electrostatic forces are used to accelerate the ion beam, there is the further possibility of modifying those forces to produce the required deflection. Three mechanisms are feasible, and all are considered below. The first involves a direct modification of the configuration of the electric field within the grids. The second achieves the same objective by moving the grids transversely with respect to each other. The third varies the extracted current density across the grids by changing their separation.

In addition, a further mechanism was considered, in which the plasma density within the discharge chamber is changed across a diameter, thereby moving radially the position of the thrust vector. This can theoretically be accomplished by altering the applied magnetic field to produce an asymmetrical discharge. Another method would be to use a segmented anode and multiple parallel anode power supplies.

Purely mechanical methods are not considered in this paper, since they represent mature technology. However, one extension of these techniques worthy of future design effort is to move the complete grid assembly with respect to the discharge chamber [5].

The frequency response achievable by the techniques considered here is more than adequate to meet real or implied requirements. Most of these techniques involve electrical actuation via simple circuits, and a time response of faster than 1 msec should be achievable. The important exceptions are the cases in which the grids are moved with respect to each other. This requires a small mechanical movement of less than 1 mm for the maximum deflection of the ion beam, which should take of the order of 1 sec at most, depending upon the method of actuation.

External Electrostatic Deflection

This very simple concept involves the passage of the beam through two pairs of orthogonal deflector plates to which high potentials are applied. These plates are shaped to maintain a constant distance from the beam, as shown in Fig 4. This shaping includes a flare along the z-axis to match the divergence of the beam, with an additional allowance to accommodate the vectoring angle required. If the beam divergence is β, which is usually of the order of 10 to 20 deg depending on operating conditions, the plates diverge at a total angle to the axis of $(\alpha + \beta)$. The deflector plates are connected to a pair of power supplies which can reverse the polarity of their outputs if necessary; this is required to change the direction of the deflection.

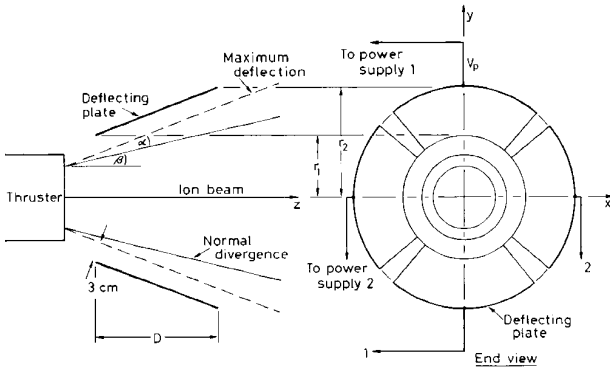

Figure 4 – Scheme for achieving electrostatic beam deflection.

This mechanical arrangement should be simple to implement, provided that the external deflecting plates are not too long; it is suggested that they cannot be significantly longer than the thruster. Another requirement is to ensure that the sputtering damage caused to the internal surfaces of the plates by ions at the periphery of the beam is acceptably small.

The remaining unknown concerns the output voltages and currents required of the power supplies. The latter should not be a problem, since current continuity demands that the electron current collected by one electrode be balanced exactly by the ion current to the other, assuming that neither are emitters. Although the electron current could be large, the ion current is restricted to that generated by charge-exchange reactions in the ion beam. As can be judged from the accel and decel grid currents of the T5 thruster [25], these are likely to be of the order of a few mA.

To assess typical potentials, it was assumed that the electrodes are separated by 3 cm from the nominal edge of the fully deflected ion beam. The electric field, E_y, then varies along their length, D, owing to their increasing separation. If a cartesian co-ordinate system is selected (Fig 4), with the origin at the centre of the upstream end of the plates, the acceleration of the ions in the direction transverse to their axial velocity is given by

$$\frac{d^2y}{dt^2} = \frac{dv_y}{dt} = \frac{eE_y}{m_i}$$

where v_y is the transverse velocity, t is time, e is the charge on an electron, and m_i is the mass of the ion, which is assumed to be singly charged. Thus

$$v_y = \frac{e}{m_i}\int_0^T E_y dt \frac{e}{m_i}\int_0^T \frac{V_p}{2r_p}dt = \frac{e}{2m_i}\int_0^T \frac{V_p}{r_1 + z\tan(\alpha+\beta)}dt$$

where V_p is the potential difference between opposite plates, r_p is their radius at axial position z, and r_1 is the value of r_p at $z = 0$. T is the time taken for the ions to traverse the full length of the plates.

Integrating, and bearing in mind that $z = v_z t$, where v_z is the axial velocity of the ions,

$$v_y = \left[\frac{eV_p}{2m_i}\frac{1}{v_z\tan(\alpha+\beta)}\log[r_1 + tv_z\tan(\alpha+\beta)]\right]_0^T$$

Noting that $v_y = v_z\tan\alpha$, this expression was used to calculate the variation of α with V_p, assuming dimensions appropriate to the T5 thruster [13], that is D = 20 cm, β = 13 deg and r_1 = 10 cm.

The results are shown in Fig 12, from which it can be seen that the deflection is almost linear with Vp and that the potential required to provide a given angle rises with increase of beam accelerating potential, V_b, and thus with v_z. Under normal operating conditions for the T5 thruster, with V_b = 1100 V and v_z = 40 km/s, a deflection of 8 deg can be obtained for a potential of just over 400 V. However, it should be noted that much higher voltages would have been derived if T6 thruster dimensions had been assumed [26], owing to the greater beam diameter.

While this is an encouraging result, which suggests that an experimental investigation of this technique might be worthwhile, two potential problems have so far been ignored. One is the formation of plasma sheaths at the internal surfaces of the deflecting plates, and the other is the possibility of arc discharges between these plates.

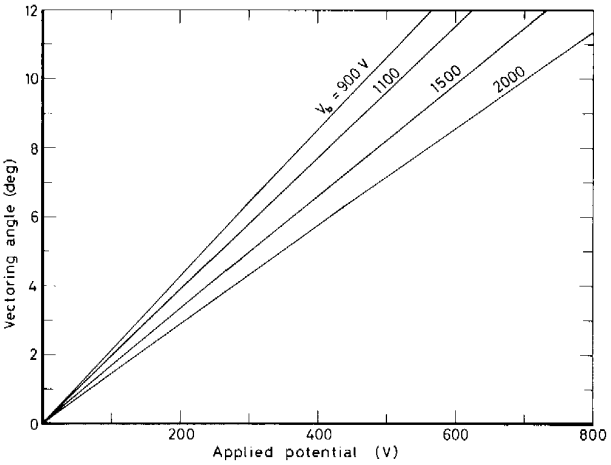

Figure 5 - Electrostatic deflection angle as a function of applied potential.

Relatively thin plasma sheaths will form if the electron number density is sufficiently high. Since much of the applied voltage will appear across them, they will distort the electric field distribution, reducing the amount of vectoring achieved for a given potential. It should be noted that the effect may be present in the laboratory, but not in space, due to the much higher background pressure in the former situation, so an experimental study of this vectoring technique may not be immediately applicable to space operation.

The sheath thickness is a few times the Debye length, λ_d. This is given in cm by the expression

$$\lambda_d = \left(\frac{kT_e}{4\pi e^2 n_e}\right)^{1/2} = 6.9\left(\frac{T_e}{n_e}\right)^{1/2}$$

in which cgs units are used. Here, k is Boltzmann's constant, T_e is the electron temperature, and n_e is the electron number density.

In the laboratory, electric probe experiments [27] have shown that typical values of T_e and n_e in the charge-exchange plasma around the central core of the ion beam from the T5 thruster are about 0.5 eV and 10^8 to 10^{10} cm^{-3}, respectively. Thus λ_d is 5×10^{-3} cm to 5×10^{-2} cm, which is very much less than the separation between the deflecting plates. It is thus clear that sheath effects will occur in the laboratory, and higher applied voltages will be necessary to achieve the desired beam deflections.

Magnetic deflection

While it is certain that the ion beam can be deflected by using a transverse magnetic field, calculations are necessary to establish how large this field would have to be to provide deflections of interest and to indicate the likely mass and power consumption of the necessary equipment. The configuration under consideration is shown in Fig 6. In this, the ion beam passes between the poles of an electromagnet designed to provide an approximately uniform field over a substantial length of the beam, just outside the grid system of the thruster. The polepieces must be separated sufficiently to avoid any direct impingement on them by high energy ions. This separation can of course vary with distance from the thruster, but this would provide a significantly non-uniform magnetic field. An electromagnet configured to provide a deflection in the perpendicular direction is also indicated in Fig 6.

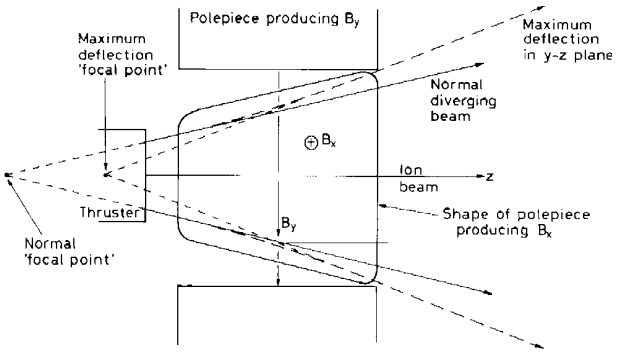

Figure 6 – External magnetic deflection configuration for one axis.

As indicated in Fig 6, the field, B_x, along the x axis this will cause the ion beam to deviate progressively from its normal direction, so that it eventually emerges from the magnetic field with the desired deflection. Reversal of the field will cause a deflection to occur in the opposite direction. Owing to the progressive nature of this process, the apparent focal point of the beam ions will move towards the grid assembly.

Assuming that the field is uniform and perpendicular to the ion motion, the ions move in an arc of a circle of radius r_g (the gyro-radius). In cgs units,

$$r_g = \frac{m_i c\left(\bar{v} \wedge \bar{B}\right)}{eB^2} = \frac{m_i v_z c}{eB_x}$$

where c is the velocity of light. This motion continues until the ions exit the field region, so that both this dimension and the magnitude of B_x determine the total deflection achieved.

Consideration of the ion trajectories leads to the following expressions, where G is the length of the interaction region along the z axis:

$$r_g = \frac{G}{\sin\alpha} = \frac{m_i v_z c}{eB_x} \quad \text{and} \quad B_x = \frac{m_i v_z c}{eG}\sin\alpha$$

Taking α = 8 deg, v_z = 40 km/s, and G = 15 cm, this gives B_x = 505 Gauss. Although large, this seems to be a practical value, warranting further investigation. It should be noted that B_x is inversely proportional to G, so reducing this dimension will increase the difficulty in producing an adequate field, although it will result in a lower polepiece mass.

The features of the magnetic circuit necessary to achieve this were evaluated, noting that the separation between the polepieces must be adequate to avoid direct ion beam impingement on them at maximum deflection. In addition, the ferromagnetic material used must have a low remanence if vectoring to all angles down to zero is to be possible. Soft iron was assumed to be used, with conservative values of permeability of 5000 and maximum flux density of 1.15×10^4 Gauss.

Taking into account the reluctance of each component, a coil of 1.4×10^4 A-turns was found to be necessary to provide B_x = 505 Gauss and a deflection of 8 deg. Thus, assuming a current of 2 A, just under 7000 turns are needed with a resistance of 68 Ω, giving a power consumption of 271 W. This must be regarded as excessive.

The mass of the iron core and energising coil were calculated to be 39 kg and 5.5 kg, respectively, giving a total of 44.5 kg, not counting support structures and power supplies. This is a prohibitively large mass, especially as it provides vectoring in one plane only and is for the relatively small T5 thruster. It can thus be concluded that this technique for thrust vectoring is theoretically possible, but that practical considerations, especially mass and power consumption, rule it out.

Electrostatic Deflection within the Grid System

Many attempts were reported in the 1970s to achieve a thrust vectoring capability using systems having low mass and power consumption, and a minimum impact on the size and shape of the thruster. As electrostatic acceleration and focusing of the ion beam are essential to these thrusters, a clear way forward was to influence these processes to provide the desired vectoring.

The approach adopted by Hughes in a NASA-funded programme [5, 7] was to build a complex accel grid in which minute secondary electrodes were inserted into the individual apertures. These were interconnected so that bias potentials could be applied to set up a transverse electric field, thereby deflecting the ion beam to the required extent. After considerable effort, success was achieved, but the sputtering processes within the grids, and the associated deposition of conducting layers, caused serious problems with leakage currents and electrical breakdowns.

A more practical solution was to use thin ceramic strips slotted together to form an interlocking structure when assembled. The electrodes were formed from a continuous molybdenum strip brazed to each side of the ceramic, resulting in a symmetrical unit from which the final assembly was constructed. This scheme gave high structural integrity and required only a few electrical connections at the periphery of the grid. A later design modification aimed to shield the downstream surfaces of the insulator strips from material back-sputtered from the ion beam target. This was accomplished by bending the downstream edges of the molybdenum strips to provide shadow shields.

To improve further the resistance to sputter deposition problems, the design was modified [5] to eliminate the ceramic strips. The electrodes were then suspended from the end supports only. However, insulators were still required there, and the longest reported test of this concept was for 100 hours. An additional change was to tension the electrode strips individually to improve their stability under thermal load, but the resulting design was very complex.

A number of different grids were fabricated and tested, formed from rectangular arrays of up to 100 holes. Despite the complexity, aperture diameters as small as 3.2 mm were feasible, with grid thicknesses in the range 2.5 to 4.5 mm. Vectoring was achieved in all 4 directions, and a linear relationship was found between deflection angle and applied potential. It became clear that this technique works very effectively, at least on small, relatively inefficient thrusters operating at high total extraction potentials (typically greater than 2 kV). However, the serious disadvantages mentioned above led to its abandonment by NASA. These problems have not diminished in severity with the passage of time, and it is not easy to see how any recent advances in technology might alleviate them.

Grid Translation

It is well known that the electrostatic field between the screen and accel grids can be modified by moving them relative to each other, thereby achieving a deflection of the ion beam. This is the principle involved in the "compensation" of the grids of the T5 Kaufman-type thruster [28]. In this, a displacement of the holes in one grid relative to the other causes an increase of divergence, reducing the focusing effect of the concave dishing of the grids and minimising overall divergence. In the optimisation of this process, a divergence of as low as 8 deg was achieved [29] with a compensation of 1%, but direct ion impingement on the accel grid caused a relaxation of this parameter to the present 0.5%.

Studies of the potential use of this mechanism for vectoring commenced in the 1960s. One of the first published accounts, from NASA Lewis [4], concerned the possible thrust vector misalignments of the beam produced by the SERT II 15 cm diameter thruster, which flew on an 11 years duration mission [30] commencing in 1969. A mathematical model was developed to predict these effects, and it was concluded that a translational movement of only 0.5 mm would vector the beam by 14 deg.

Other theoretical work [7] showed that direct ion beam impingement on the accel grid is a fundamental limitation of this process, especially at high extracted current density. In the case studied, a deflection of 6 deg caused direct impingement at high current density, but some reduction in this parameter permitted 10 deg to be achieved. These values were confirmed by experimentally.

Early experiments were conducted using a variety of mechanical methods for controlling the transverse positions of the grids, while accurately maintaining axial separation. For example, Hughes [5] employed 8 carefully matched coil springs pulling the screen grid in mutually perpendicular directions. In this concept, the screen grid was supported axially by the outer polepiece when under axial loads. However, four thin flexible columns were also provided which normally defined the axial separation from the accel grid.

The springs were made of a cobalt-nickel alloy which retained its mechanical characteristics up to a temperature of 600° C. Heating the springs selectively in pairs permitted translation of the screen grid with respect to the accel, a movement of 2.2 mm being measured for a temperature differential of 200° C and a power dissipation of 3.5 W in air. It was found that the maximum deflection obtainable from the 5 cm

diameter thruster was more than 21 deg. The design goal of 10 deg was achieved with a power dissipation of 1.1 W. The maximum deflection recommended above, 8 deg, was accomplished with a translation of 0.24 mm, or 10% of the screen grid aperture diameter.

Although resistance to launch vibration was not covered, the disadvantage of a very long time constant was recognised [5]. This resulted from the use of a thermal actuation system. The time required to achieve a deflection of 10 deg was 10 min if only the steady-state deflection power was applied, and the return to zero deflection required about 30 min. Both times were improved to about 1 min by over-powering when applying the deflection, and by heating opposing springs to the same temperature and allowing both sets to cool at the same rate when returning to zero.

A satisfactory life test of this system of more than 2000 hours was conducted at NASA Lewis Research Center [31] using a different 5 cm diameter thruster, with the beam deflected by 10 deg for most of this time. An extrapolated grid lifetime of better than 10,000 hours, possibly as much as 20,000 hours, was predicted from the results obtained.

A translational vectoring system was also designed for the NASA/Hughes 30 cm diameter thruster [31,32], which incorporated flat grids. This followed the same principles, but utilising three pairs of springs, necessitated by the use of 12 grid mounting points, and stiffer axial support rods were needed to cater for the increased mass of the screen grid. A central inter-grid support spacer was also introduced.

A theoretical analysis was undertaken [33] of the capabilities and limitations of this system, including its application to outwardly dished grids. The beam deflection angle was found to be relatively invariant with respect to beam current, but to be strongly dependent upon inter-grid spacing; larger deflections were obtained for closer spacings. However, the maximum deflection obtainable before the onset of direct ion impingement fell rapidly with increase of beam current. As regards dishing, no problems were found in this study, and it was predicted that deflections as great as 20 deg might be achievable by suitable design. The potential problems towards the periphery of the grids, caused by the change in spacing as the grids move relative to each other, are alleviated by the lower plasma and ion current densities. It was concluded that a 10 deg beam deflection from the 30 cm thruster could be obtained with a relative motion of 10% of the screen grid hole diameter.

A further experimental and theoretical study by Homa and Wilbur [6] confirmed most of the earlier work, and suggested that grid translation is, in principle, a viable procedure. It was also confirmed that the useful vectoring range is limited by the onset of direct impingement, which is most severe at high current density and with small accel grid holes. Over this range, which is also dependent upon the net to total voltage ratio, the total accelerating voltage, the grid separation, and the grid thicknesses, the deflection is proportional to the translation distance. There is no effect on beam divergence.

In view of these encouraging results from earlier work, simple calculations were made of the vectoring capability of the grids of the T5 and T6 thrusters, provided that a suitable actuation system can be designed. In this, it was assumed that the accel grid is moved laterally by a distance ε, which corresponds to an angular movement, as defined in Fig 7, of ρ. Using the physical dimensions of the grids defined in Fig 7,

$$\rho = \tan^{-1}\frac{\varepsilon}{l_a + t_s + t_a}$$

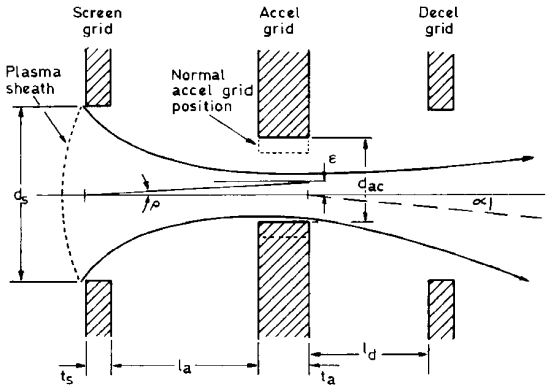

Figure 7 – Translational vectoring with a triple-grid system.

The deflection of a beamlet can be estimated using linear particle optics theory [34], regarding the accel grid aperture as a thin lens with focal length h. Making this assumption,

$$h = 4\frac{V_T}{E_2 - E_1}$$

where $V_T = V_b + |V_{ac}|$, V_{ac} is the accel grid potential, and E_1 and E_2 are the electric fields on the acceleration and deceleration sides of the accel grid, respectively. In addition, the vectoring angle is given by $\alpha = \varepsilon / h$.

In the absence of experimental data concerning electric field distributions, the values of E_1 and E_2 can be obtained approximately from

$$E_1 = \frac{V_b + |V_{ac}|}{l_a} \quad \text{and} \quad E_2 = \frac{|V_{ac}| - |V_{dec}|}{l_d}$$

where V_{dec} is the decel grid potential, and l_a and l_d are defined in Fig 7. These expressions should be reasonably valid in the uniform field region away from the edges of the grids. They allow α to be calculated using the following equation, which is obtained by combining the above relationships. Thus

$$\alpha = \frac{-\varepsilon}{4}\left(\frac{E_1 - E_2}{V_b - |V_{ac}|}\right)$$

where the negative sign indicates that the deflection is in the opposite direction to the grid displacement.

This confirms that α is directly proportional to ε, as found in earlier experiments [5]. Since E_1 and E_2 have opposite signs, the deflection is greater if E_2 is significant. The approximate nature of the analysis is indicated by the absence of any explicit dependence of α on the other geometrical parameters defined in Fig 7. Although this deficiency can be rectified by more exact treatments [35], the trends indicated above have been confirmed by experiment [6], so this treatment is deemed to be adequate for the present purposes.

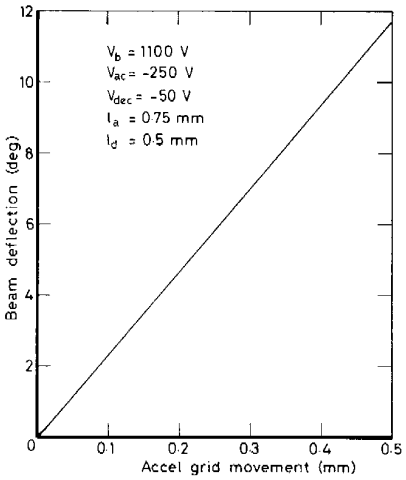

Figure 8 – Ion beam deflection as a function of accel grid displacement.

Using the above expressions, the results presented in Fig 8 were obtained. These are applicable to both the T5 and T6 thrusters, since the geometrical configurations of the grids are identical in these two devices. It can be seen that a beam deflection of 8 deg, for which ρ = 9.7 deg, is predicted for a translation of 0.34 mm. This is 16% of the diameter of the screen grid holes, 2.15 mm, and is a movement which should be practical to implement.

As an illustration of the dependence of the magnitude of the deflection on other parameters, the effects of changing V_{ac} and l_a are illustrated in Fig 22. It can be seen that an 8 deg deflection is obtainable for translational movements of between 0.31 and 0.35 mm as V_{ac} is reduced from 400 to 200 V. Thus the usual aim of minimising V_{ac} necessitates a slightly higher grid movement in order to achieve the same beam deflection.

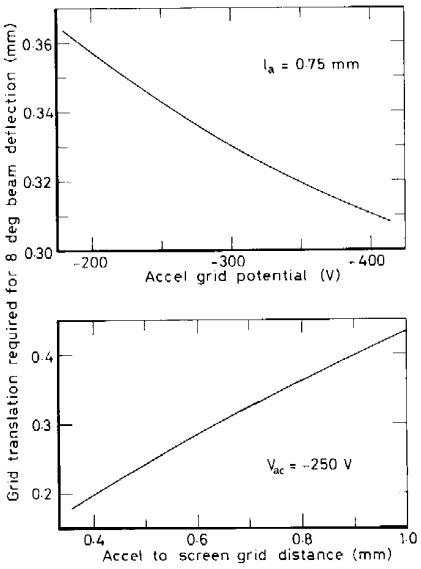

Figure 9 – Dependence of accel grid translation distance on grid potential and accel to screen grid separation for α = 8 deg.

The situation is much the same as regards changes in l_a. For the range 0.4 to 1.0 mm, the grid translation required to provide a deflection of 8 deg varies from 0.2 to 0.43 mm, which again is acceptable. However, this variation does indicate a potential problem which must be addressed in an actual design exercise. This concerns the variation of l_a over the surface of the grid due to manufacturing errors. Should this be significant, it will cause the beam deflection resulting from a given translational movement to vary with position, effectively increasing the beam divergence.

Another factor not so far considered is the maximum deflection available before direct ion impingement on

the accel grid occurs. As the diameter of a beamlet in an individual aperture of the grid assembly depends on the current density drawn through it [25], the ions are very close to the edge of the accel grid holes when the beamlet current is high, and virtually no beam deflection is possible. Conversely, a lower current density situation permits a considerable vectoring angle to be achieved. This is the primary limitation to the effectiveness of this vectoring technique.

For example, at and near the centre of the grids of the T5 thruster when configured to operate at 25 mN no vectoring is possible, without de-rating the thrust to a lower value. A compromise is necessary between the need to achieve the maximum thrust density and any thrust vectoring requirements that may be specified. However, these limitations can be alleviated to some extent by modifying the thruster to exhibit a relatively flat plasma density profile [29].

It can be concluded that this is a viable thrust vectoring technique, provided that the obvious mechanical problems can be solved. The amount of grid movement required to provide vectoring angles of interest are not excessive, even when large ranges of accel grid potential and screen to accel grid separation are considered. However, the limitations on vectoring angle imposed by direct ion beam impingement on the accel grid must be studied in detail, taking into account the plasma density distribution in the discharge chamber.

Variation of Grid Separation

The maximum current that can be extracted through a single grid aperture depends on its perveance, μ_p. This is defined by the expression

$$\mu_p = \frac{I_h}{\left(V_b + |V_{ac}|\right)^{3/2}} = \frac{I_h}{{V_T}^{3/2}}$$

where I_h is the ion current carried by an individual beamlet. This is derived from an analysis in which the current limit is set by the Child-Langmuir solution to the inter-grid electric field configuration.

This approach leads to the equations

$$\mu_p = \frac{4\varepsilon_o}{9}\left(\frac{2e}{m_i}\right)^{1/2}\frac{A_h}{{d_a}^2} \text{ and } I_h = \frac{4\varepsilon_o}{9}\left(\frac{2e}{m_i}\right)^{1/2}\left(V_T\right)^{3/2}\frac{A_h}{{d_a}^2}$$

where mks units are used, ε_o is the dielectric constant of free space, and A_h is the effective area of the plasma sheath emitting ions into the aperture. The actual ion acceleration length, d_a, is given approximately by

$$d_a = l_a + t_s + 0.5t_a$$

This ignores the contribution made to d_a by the penetration of the plasma sheath into the discharge chamber of the thruster, as indicated in Fig 7.

While under normal circumstances only the centre of the grids will operate at maximum perveance, the above expressions indicate the relationships between the parameters which influence the ion extraction process. In particular, any variation of l_a will cause the extracted current to change according to an approximately inverse square law relationship. It would therefore appear to be feasible to alter the extracted ion current density distribution across the grid system by modifying l_a. This will result in a radial movement of the thrust vector, thereby achieving a vectoring capability, although with the disadvantage of a decrease in actual thrust.

The effectiveness of this technique was assessed by considering a set of grids in which the screen to accel separation at the end of a diameter is increased by a factor λ, as indicated in Fig 10. If the distance along the diameter is x, with the zero at the position where there is no change in separation, the increase in separation is directly proportional to x.

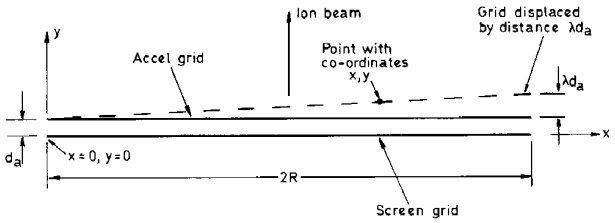

Figure 10 – Vectoring by displacement. of the accel grid in the axial direction.

If the axial displacement of the accel grid from the emitting sheath at x is denoted by y, and generalising the above expressions to apply to any surface area of the grids, the maximum thrust, δF_e, from an elementary area, δA_e , will be given by

$$\delta F_e = \delta I_e\left(\frac{2V_b m_i}{e}\right)^{1/2}$$
$$= \frac{8\varepsilon_o}{9}\left(V_b\right)^{1/2}\left(V_T\right)^{3/2}\frac{\delta A_e}{y^2} = \frac{8\varepsilon_o}{9}\left(V_b\right)^{1/2}\left(V_T\right)^{3/2}\frac{w\delta x}{y^2}$$

where δI_e is the current emitted by the elementary area of width w. If R is the grid radius,

$$y = d_a + \frac{\lambda d_a x}{2R}$$

As defined earlier, the total additional grid separation at the edge, where $x = 2R$, is then λd_a.

As the effect will follow the same relationship along any chord of the grids parallel to this diameter, the change in the position of the thrust vector can be assessed from its position along this narrow strip only. The total thrust, F_s, produced by it is then

$$F_s = \frac{8\varepsilon_o}{9}(V_b)^{1/2}(V_T)^{3/2} w \int_0^{2R} \frac{dx}{y^2}$$

and its moment about the edge of the grid, where $x = 0$, is $x_m F_s$, where x_m is the position of the effective thrust vector along the diameter.

This moment may also be calculated by summing the individual moments of the elementary areas considered above. This is

$$\int_0^{2R} x\delta F_e = \frac{8\varepsilon_o}{9}(V_b)^{1/2}(V_T)^{3/2} w \int_0^{2R} \frac{x}{y^2} dx$$

The two expressions above for the total moment may be equated to solve for x_m. Substituting for y, and using the additional substitution $x' = 2R + \lambda x$, integration of this equality eventually yields

$$x_m = \frac{2R}{\lambda}\left[\frac{1+\lambda}{\lambda}\log_e(1+\lambda) - 1\right]$$

noting that for $x = 0$, $x' = 2R$, and that for $x = 2R$, $x' = 2R(1+\lambda)$. As expected, x_m depends only upon R and λ since, within the approximations involved in the above analysis, the potentials applied to the grids and the actual current drawn do not affect the results

This expression was used to provide the graph of thrust vector movement against λ presented in Fig 11 for the T5 thruster. This shows that movements of up to about 2 cm are feasible, although the values of λ required exceed 2 and will result in a substantial decrease in the total perveance of the grid system, and therefore of the maximum available thrust.

Over a typical thruster lifetime of 10^4 hours, assuming operation at the Artemis thrust value of 18 mN, a maximum total angular impulse of 1.3×10^4 Nsm would be generated with a thrust vector displacement of 2 cm. This could be a valuable contribution towards the corrections required to compensate for thrust vector misalignments, thrust imbalances and restricted movements of the CoM of the satellite.

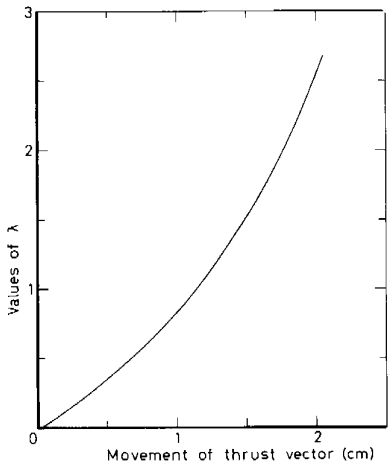

Figure 11 – Radial movement of thrust vector as function of λ.

Plasma Density Modulation

Modification of the plasma density profile in the discharge chamber to achieve a vectoring capability avoids the potential reliability problems inherent in mechanical systems. In principle, it is similar to altering the grid separation, in that the position of the thrust vector is changed to provide a moment which can be used to correct the attitude of the spacecraft. Two methods are available to modulate the plasma density profile so that it becomes asymmetrical, in essence by altering the distribution of the flux of primary electrons within the discharge chamber. This can be done by modifying either the magnetic field or the distribution of the discharge current.

In the case of the magnetic field, an obvious strategy is to control the currents through the individual solenoids independently. This can be done by using separate power supplies, or by operating them in parallel from a single supply, but with a current controlling element in series with each solenoid. No mechanical changes are needed, but additional circuitry within the PCCE will be necessary. Power consumption will also be increased marginally, as will total mass.

The use of an asymmetrical discharge current is probably the most direct and easily analysed option. Unfortunately, it requires modification to the anode to form an azimuthally segmented structure, with all segments insulated from each other. Possible 6 or 8 segments would be required, insulated from each other and from the discharge chamber. As with the solenoids, these segments would have to be

independently supplied with current, either using separate power supplies, or a single supply could be utilised with independent controlling elements in the circuits leading to the different segments.

The possible moment that might be achieved in this way depends critically on how asymmetrical the discharge can become before severe instabilities appear. The preceding analysis on the effects of changes to the screen to accel grid separation give some guide to the possible outcome, since the mechanism, that of moving the position of the thrust vector, is the same in both cases. A qualitative estimate suggests that an offset of perhaps 20% of the beam diameter might be achieved. This would be about 2 cm in the case of the T5 thruster, with the T6 giving 4 to 5 cm.

It should be emphasised that this approach has never been subjected to an experimental or theoretical assessment from which to judge the viability of the concept. All previous work has been directed to ensuring the best possible azimuthal symmetry in the discharge chamber, to maximise the stable operating range of the thruster. Moreover, as far as is known, no work has been done to establish how much asymmetry can be introduced before unacceptable instabilities are generated. Thus, although this concept is very attractive from the viewpoint of the avoidance of active mechanical systems, much experimental work will be necessary before a judgement will be possible as to its viability.

Conclusions

The attitude and orbit control of geostationary communications satellites is a complex task often employing numerous chemical thrusters, as well as devices such as momentum wheels. The associated propellant consumption is of serious concern, since it adds considerably to launch costs, so anything which affects this significantly is of importance. One such factor is the utilisation of ion engines for station-keeping, since any misalignment of their thrust vectors with respect to the centre of mass of the spacecraft can add to the attitude and orbit control requirements. This paper considers the possible perturbations that might result from such effects, and evaluates the different methods available to provide compensation via active thrust vectoring.

The paper reports the results of a study of the implications of thrust vector misalignments of gridded ion thrusters. It is shown that orbital disturbances will be negligible and that attitude corrections will require only a small and acceptable expenditure of propellant. However, movements of the centre of mass of the spacecraft during operation, together with uncertainties in its initial position, are very significant and may lead to large and unacceptable propellant consumptions. It is concluded that a thrust vectoring capability of about 8 to 10 degrees should be provided if ion engines are used for north-south station-keeping.

The paper then considers the possible methods by which this vectoring might be achieved, excluding the existing mechanical systems. External electrostatic or electromagnetic deflection of the emerging ion beam is shown to be technically feasible, but the mass of the hardware required in the latter case will be prohibitive. Electrostatic deflection of the ions within the extraction grid system is found to be much more promising. The preferred method involves a lateral relative translation of the accelerator and screen grids, a movement of under 0.5 mm producing the desired beam deflection of 8 to 10 degrees.

Other methods examined in the paper include two by which the thrust vector is moved along a specified radius of the grid, rather than being deviated through an angle. The first of these requires the separation between the accelerator and screen grids to be changed by tilting one with respect to the other. The second concept depends on achieving an azimuthal variation of the plasma density within the discharge chamber, which can be realised by a variety of discharge modulation processes.

It is concluded that the most promising option is to use electrostatic deflection of the ions within the grid system, by lateral translation of the accel grid with respect to the screen grid.

References

[1] Fearn, D G, “Electric propulsion of spacecraft”, *J Brit Interplan Soc*, 35, 156-166, (1982).

[2] Renault, H, Silvi, M, Bohnhoff, K and Gray, H, “Electric propulsion on ARTEMIS: a development status”, Proc *Second European Spacecraft Propulsion Conf*, Noordwijk, Holland, 27-29 May 1997. ESA SP-398.

[3] Anzel, B, “Stationkeeping the Hughes HS 702 satellite with a xenon ion propulsion system”, IAF Paper IAF-98-A.1.09, (September/October 1998).

[4] Lathem, W C, “Approximate analysis of the effects

of electrode misalignments on thrust vector control in Kaufman thrusters, AIAA Paper 68-89, (January 1968).

[5] Collett, C R, King, H J and Schnelker, D E, “Vectoring of the beam from ion bombardment thrusters”, AIAA Paper 71-691, (June 1971).

[6] Homa, J M and Wilbur, P J, “Ion beamlet vectoring by grid translation”, AIAA Paper 82-1895, (November 1982).

[7] King, H J and Schnelker, D E, “Thrust vectoring systems”, AIAA Paper 70-1150, (August/September 1970).

[8] Rees, T and Fearn, D G, "Use of the UK 10 cm ion thruster for north-south station-keeping of the proposed European TVBS spacecraft", AIAA Paper 76-1059, (November 1976).

[9] Day, M L, Colbert, T S, Marx, S H and Ozkul, A, "Intelsat VII ion propulsion subsystem implementation study", AIAA Paper 90-2550, (July 1990).

[10] Fearn, D G and Smith, P, "The application of ion propulsion to Intelsat VII class spacecraft", AIAA Paper 89-2275, (1989).

[11] Ryden, K A and Fearn, D G, "End-of-life disposal of satellites using electric propulsion: an aid to mitigation of the space debris problem", IAF Paper 95-IAA.6.5.04, (October 1995).

[12] Fearn, D G, “The interactions between a T5 ion thruster and a host spacecraft”, Proc Second European Spacecraft Propulsion Conference, ESTEC, Noordwijk, Holland, 27-29 May 1997. ESA SP-398, (1997).

[13] Fearn, D G and Smith, P, “A review of UK ion propulsion - a maturing technology”, IAF Paper IAF-98-S.4.01, September/October 1998).

[14] Nagama, D, "Development of the ion propulsion system for ETS-VI", Proc Intelsat Symposium on Electric Propulsion, Sacramento, 28 June 1991.

[15] Bohnhoff, K and Bassner, H, “Commercialized ion propulsion for north/south station keeping of communication satellites”, Proc Second European Spacecraft Propulsion Conference, ESTEC, Noordwijk, Holland, 27-29 May 1997. ESA SP-398, (1997).

[16] Porte, F, Saint Aubert, P, Mawby, D and Hsing, J, "Application of ion propulsion system to communications spacecraft", IEPC Paper 93-015, (September 1993).

[17] Pollard, J E, Jackson, D E, Marvin, D C, Jenkin, A B and Janson, S W, "Electric propulsion flight experience and technology readiness", AIAA Paper 93-2221, (June 1993).

[18] Pye, J W, "UK, T5 ion engine thrust vector control considerations", AIAA Paper 76-1064, (1976).

[19] Sachdev, D K, "Historical overview of the Intelsat system", *J Brit Interplan Soc,* 43, 8, 331-338, (1990).

[20] Templeton, L W, "Intelsat VII overall spacecraft design", Proc IEE Colloquium on "Intelsat VII - another Step in the Evolution of the Global Intelsat Communications System", London, 23 March 1989. IEE Digest 1989/48.

[21] Pollard, J E, “Beam-centroid tracking instrument for ion thrusters”, *Rev Sci Instrum*, 65, 3733, (1994).

[22] Mundy, D H and Fearn, D G, “Throttling the T5 ion engine over a wide thrust range”, AIAA Paper 97-3196, (July 1997).

[23] Mundy, D H, “T5 ion engine plume analysis using a time of flight mass spectrometer”, IEPC Paper 97-096, (August 1997).

[24] Fearn, D G, " The proposed demonstration of the UK-10 ion propulsion system on ESA's SAT-2 spacecraft", IEPC Paper 88-031, (October 1988).

[25] Bond, R A, Fearn, D G, Wallace, N C and Mundy, D H, “The optimisation of the UK-10 ion thruster extraction grid system”, IEPC Paper 97-138, (1997).

[26] Wallace, N C, Mundy, D H and Fearn, D G, “A review of the development of the T6 ion thruster system”, IAF Paper IAF-99-S.4.08, (October 1999).

[27] de Boer, P C T, “Measurement of electron density in the charge exchange plasma of an ion thruster”, J Propulsion and Power, 13, 6, 783-788, (Nov-Dec 1997).

[28] Wells, A A, “Current flow across a plasma “double layer” in a hollow cathode ion thruster”, AIAA Paper 72-418, (April 1972).

[29] Fearn, D G, Stewart, D, Harbour, P J, Davis, G L and Williams, J, “The UK 10 cm mercury ion thruster development program”, AIAA Paper 75-389, (1975).

[30] Kerslake, W R, “SERT II thrusters - still ticking after eleven years”, AIAA Paper 81-1539, (July 1981).

[31] Lathem, W C, “Grid-translation beam deflection systems for 5-cm and 30-cm diameter Kaufman thrusters”, AIAA Paper 72-485, (April 1972).

[32] King, H J and Poeschel, R L, “:Low specific impulse ion engine”, Hughes Research Laboratories, Final Report on NASA Contract NAS 3-11523, NASA CR-72677, (February 1970).

[33] Lathem, W C and Adam, W B, “Theoretical analysis

of a grid-translation beam deflection system for a 30-cm diameter Kaufman thruster", NASA TM X-67911, (August 1971).

[34] Whealton, J H, "Linear optics theory of ion beamlet steering", Rev Sci Instrum, 48, 11, 1428-1429, (1977).

[35] Harbour, P J, "Charge-exchange and beam bending at extraction electrodes", Proc 3rdEuropeanElectric Propulsion Conf, Hinterzarten, Germany, October 1974. DGLR Fachbuchreihe Band 5, pp 270-275, (1974).